INTERNATIONAL JOURNAL FOR NUMERICAL METHODS IN ENGINEERING, VOL. 21, 1013–1025 (1985)

THE COMPLEX VARIABLE BOUNDARY ELEMENT METHOD: APPLICATIONS

T. V. HROMADKA II[†]

U.S. Geological Survey, Laguna Niguel, California, U.S.A.

C. C. YEN[‡] AND G. L. GUYMON[§]

University of California, Irvine, California, U.S.A.

SUMMARY

The complex variable boundary element method (CVBEM) is used to approximate several potential problems where analytical solutions are known. A modelling result produced from the CVBEM is a measure of relative error in matching the known boundary condition values of the problem. A CVBEM error-reduction algorithm is used to reduce the relative error of the approximation by adding nodal points in boundary regions where error is large. From the test problems, overall error is reduced significantly by utilizing the adaptive integration algorithm.

INTRODUCTION

Use of complex variable theory for developing approximations for potential problems has received some renewed interest in the past few years. Hunt and Isaacs[1] and Hromadka and Guymon[2] use a boundary integral formulation to study boundary value problems of the Laplace equation. Hromadka and Guymon[3] generalized the boundary integral approach into a complex variable boundary element method (CVBEM) which has direct analogies to the well-known real variable modelling techniques. In another paper, Hromadka and Guymon[4] utilize a relative error measure to reduce the overall CVBEM modelling error by using adaptive integration techniques.

In this paper, the CVBEM will be applied to several potential problems where analytical solutions exist. In this manner, the success of the CVBEM error-reduction approach can be examined. Continuity, analyticity and convergence properties of the CVBEM approximation function are briefly discussed by expanding the resulting approximation function into a finite series of products of complex polynomials with logarithm functions.

CVBEM DEVELOPMENT

Let Γ be a simply-connected contour composed of straight-line segments. Let Ω be the simple-closed interior of Γ. Subdivide Γ into m complex variable boundary elements (CVBE) by

$$\Gamma = \bigcup_{j=1}^{m} \Gamma_j \tag{1}$$

[†] Hydrologist.
[‡] Graduate Student.
[§] Professor of Civil Engineering.

0029–5981/85/061013–13$01.30

Received 11 January 1984
Revised 15 June 1984

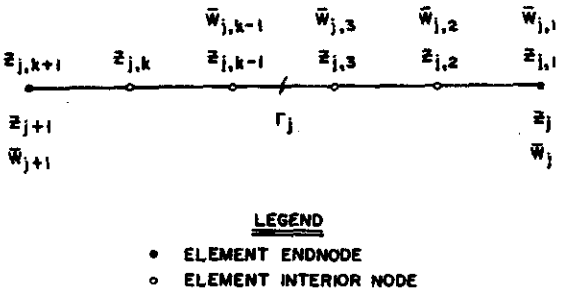

Figure 1. $(k+1)$-Node boundary element Γ_j nodal definitions

On each Γ_j define $(k+1)$ equidistant nodal points such that $z_{j,1}$ and $z_{j,k+1}$ are the endpoints of Γ_j. Figure 1 shows the global and local nodal number conventions. The global nodal co-ordinates are related to local nodal co-ordinates by $z_{j,1} = z_j$ and $z_{j,k+1} = z_{j+1,1} = z_{j+1}$. Define complex numbers $\bar{\omega}_{ji}$ at each node z_{ji}. Then order k complex polynomials $P_j^k(z)$ are uniquely defined on each Γ_j.

An order k global trial function is defined by

$$G_k(z) = \sum_{j=1}^{m} \delta_j P_j^k(z), z \in \Gamma \tag{2}$$

where

$$\delta_j = \begin{cases} 1, & z \in \Gamma_j. \\ 0, & \text{otherwise} \end{cases} \tag{3}$$

Then $G_k(z)$ is continuous on Γ and

$$\lim_{\max|\Gamma_j| \to 0} G_k(z) = \omega(z) \tag{4}$$

where in (4) it is assumed that $\omega(z)$ is analytic on $\Omega \bigcup \Gamma$ and that each $\bar{\omega}_{ji} = \omega(z_{ji})$.

Consider the H_k approximation function $\hat{\omega}_k(z)$ defined by

$$\hat{\omega}_k(z) = \frac{1}{2\pi i} \int_\Gamma \frac{G_k(\zeta)\mathrm{d}\zeta}{\zeta - z}; \quad z \notin \Gamma, z \in \Omega \tag{5}$$

Using (4)

$$\int_\Gamma \frac{G_k(\zeta)\mathrm{d}\zeta}{\zeta - z} = \int_\Gamma \frac{\Sigma \delta_j P_j^k(\zeta)\mathrm{d}\zeta}{\zeta - z} = \sum \int_{\Gamma_j} \frac{P_j^k(\zeta)\mathrm{d}\zeta}{\zeta - z} \tag{6}$$

On each Γ_j, define a local co-ordinate system by

$$\zeta_j = z_{j,1} + (z_{j,k+1} - z_{j,1})s_j; \zeta_j \in \Gamma_j, 0 \leqslant s_j \leqslant 1 \tag{7}$$

Then

$$\zeta_j = \zeta_j(s_j) = z_j + (z_{j+1} - z_j)s_j; \zeta_j \in \Gamma_j, 0 \leqslant s_j \leqslant 1 \tag{8}$$

$$\int_{\Gamma_j} \frac{P_j^k(\zeta_j)\mathrm{d}\zeta_j}{\zeta_j - z} = \int_{\Gamma_j} \frac{P_j^k(s_j)\mathrm{d}s_j}{s_j - \gamma_j} \tag{9}$$

where $P_j^k(s_j) = P_j^k(\zeta_j(s_j))$, and

$$\gamma_j = (z - z_j)/(z_{j+1} - z_j) \tag{10}$$

Equation (9) is solved by factoring $(s_j - \gamma_j)$ from $P_j^k(s_j)$. Let $P_j^k(s_j)$ be of the form

$$P_j^k(s_j) = \sum_{i=0}^{k} a_{ji} s_j^i, \quad 0 \leqslant s_j \leqslant 1 \tag{11}$$

where the a_{ji} are complex constants.

Dividing $P_j^k(s_j)$ by $(s_j - \gamma_j)$ gives

$$\int_{s_j=0}^{1} \frac{P_j^k(s_j)}{s_j - \gamma_j} \, ds_j = R_j^{k-1}(z) + P_j^k(\gamma_j) H_j \tag{12}$$

where $R_j^{k-1}(z)$ is a $k-1$ order complex polynomial; $P_j^k(\gamma_j)$ is the order k polynomial of (11) with γ_j substituted into the argument; and

$$H_j = \ln\left[\frac{z_{j+1} - z}{z_j - z}\right] = \ln\left[\frac{d_{j+1}(z)}{d_j(z)}\right] + i\theta_{j+1,j}(z) \tag{13}$$

In (13), $d_j(z) = |z - z_j|$, and $\theta_{j+1,j}(z)$ is the central angle between points z_j, z_{j+1}, z (see Figure 2). For example, let $P_j^k(s_j)$ be the order 3 polynomial

$$P_j^3(s_j) = a_{j3} s_j^3 + a_{j2} s_j^2 + a_{j1} s_j + a_{j0} \tag{14}$$

Then

$$\frac{P_j^3(s_j)}{s_j - \gamma_j} = [a_3 s_j^2 + (a_3\gamma_j + a_2)s_j + (a_3\gamma_j^2 + a_2\gamma_j + a_1)] + [(a_3\gamma_j^3 + a_2\gamma_j^2 + a_1\gamma_j + a_0)/(s_j - \gamma_j)] \tag{15}$$

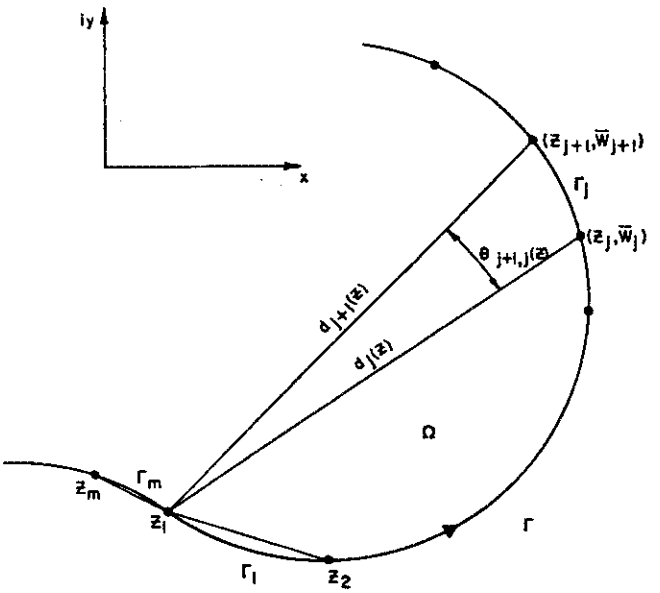

Figure 2. CVBEM linear trial function geometry

and

$$\int_0^1 \frac{P_j^3(s_j)\mathrm{d}s_j}{s_j-\gamma_j}=\left[\frac{a_3}{3}+\frac{(a_3\gamma_j+a_2)}{2}+(a_3\gamma_j^2+a_2\gamma_j+a_1)\right]$$
$$+[(a_3\gamma_j^3+a_2\gamma_j^2+a_1\gamma_j+a_0)]H_j=R_j^2(z)+P_j^3(\gamma_j)H_j \tag{16}$$

Summing the m CVBE contributions gives from (5) and (6),

$$2\pi i\hat{\omega}_k(z)=\sum R_j^{k-1}(z)+\sum P_j^k(\gamma_j)H_j \tag{17}$$

Letting $R^{k-1}(z)=(1/2\pi i)\sum R_j^{k-1}(z)$, (17) is simplified to

$$\hat{\omega}_k(z)=R^{k-1}(z)+\frac{1}{2\pi i}\sum P_j^k(\gamma_j)H_j \tag{18}$$

In (18), it is noted that the $P_j^k(\gamma_j)$ are of the form of the assumed trial functions on each Γ_j.

Letting node z_1 be on the branch cut of the complex logarithm function $\ln(z-\zeta)$, where $z\in\Omega$ and $\zeta\in\Gamma$ (see Figure 3), then (18) can be expanded as

$$\hat{\omega}_k(z)=R^{k-1}(z)-\frac{1}{2\pi i}\sum\Delta_j^{k-1}(z-z_j)\ln(z-z_j)+P_m^k(z) \tag{19}$$

where Δ_j^{k-1} is an order $(k-1)$ polynomial defined by

$$\Delta_j^{k-1}=\frac{(P_j^k(\gamma_j)-P_{j-1}^k(\gamma_{j-1}))}{(z-z_j)} \tag{20}$$

and $\ln(z-z_j)$ is the principal value. From the continuity of $G^k(\zeta)$, it is seen that, at nodal coordinate z_j,

$$P_j^k(\gamma_j)-P_{j-1}^k(\gamma_{j-1})=0 \tag{21}$$

and that $(z-z_j)$ is a factor as shown in (20). In (19), the $P_m^k(z)$ term appears due to the circuit around the branch point of the multiple valued function, $\ln(z-\zeta)$.

Letting $R^k(z)=R^{k-1}(z)+P_m^k(z)$, then

$$\hat{\omega}_k(z)=R^k(z)-\frac{1}{2\pi i}\sum_{j=1}^{m}\Delta_j^{k-1}(z-z_j)\ln(z-z_j) \tag{22}$$

Examining (22), it is seen that $\hat{\omega}_k(z)$ is continuous throughout the entire domain Ω and has

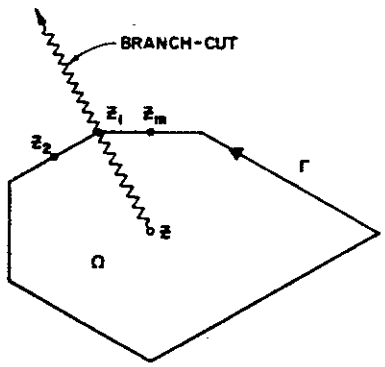

Figure 3. Branch-cut of $\ln(z-\zeta)$ function, $\zeta\in\Gamma$

removable singularities at each CVBE endpoint nodal co-ordinate $z_j, j = 1, 2, \ldots, m$. That is, $R^k(z)$ and Δ_j^{k-1} are continuous complex polynomials, and

$$\lim_{z \to z_j} (z - z_j) \ln (z - z_j) = 0 \tag{23}$$

Additionally, $\hat{\omega}_k(z)$ is analytic on Ω. Thus

$$\hat{\omega}_k(z) = \hat{\phi}(z) + i\hat{\psi}(z) \tag{24}$$

where $\hat{\phi}(z)$ and $\hat{\psi}(z)$ are two-dimensional potential and stream functions which solve the Laplace equation exactly on Ω. Thus, by forcing the approximation values of $\hat{\omega}_k(z)$ to be arbitrarily close (ε) to the boundary condition values of $\omega(z)$ on Γ, then it is guaranteed by the maximum modulus theorem that the approximation of $\omega(z)$ is bounded by

$$|\omega(z) - \hat{\omega}(z)| \leqslant \varepsilon, \quad z \in \Omega \tag{25}$$

The CVBEM proceeds by solving[3] either the integral equation of (6) in terms of nodal values $\bar{\omega}_{ji} = \bar{\phi}_{ji} + i\bar{\psi}_{ji}$, or by solving for the coefficients of the expansion of $\bar{\omega}_k(z)$ given in (22).

APPLICATIONS

Because the CVBEM produces an exact solution to the governing partial differential equation on Ω, then convergence of $\hat{\omega}_k(z)$ to $\omega(z)$ is achieved on $\Omega \bigcup \Gamma$ by forcing convergence on Γ. This is shown in a straightforward manner (without proof) by noting that from (4),

$$\lim_{\max|\Gamma_j| \to 0} \int_\Gamma \frac{G_k(\zeta)\mathrm{d}\zeta}{\zeta - z} = \int_\Gamma \frac{\lim\limits_{\max|\Gamma_j| \to 0} G_k(\zeta)\mathrm{d}\zeta}{\zeta - z} = \int_\Gamma \frac{\omega(\zeta)\mathrm{d}\zeta}{\zeta - z} = 2\pi i \omega(z) \tag{26}$$

However, we are limited to a finite number of nodal points on Γ. Therefore from (22), if $\omega(z)$ is not an order k (or less) polynomial, then

$$E(z) = R^k(z) - \hat{\omega}_k(z) = \frac{1}{2\pi i} \sum_{j=1}^{m} \Delta_j^{k-1} (z - z_j) \ln (z - z_j) \tag{27}$$

and a residual error $E(z)$ is defined by (27) to be minimized on Γ. One method of reducing $E(z)$ on Γ is to compare the known boundary condition values of $\omega(z_j)$ on Γ to the approximation values $\hat{\omega}(z_j)$ and locate regions of large deviation.[4] Additional nodal points are then defined along these large relative error locations.

To demonstrate the application of the CVBEM in determining a high precision approximation, several potential problems are examined. The applications assume that, at each nodal point, either $\bar{\phi}$ or $\bar{\psi}$ is specified (not both) and, consequently, part of the problem is to determine these unknown nodal values.

Thus for $\omega(z)$ analytic on $\Omega \bigcup \Gamma$, let $\bar{\omega}_{ji} = \omega(z_{ji})$ which implies $\bar{\phi}_{ji} + i\bar{\psi}_{ji} = \phi_{ji} + i\psi_{ji}$. But only one value of $\bar{\phi}_{ji}$ or $\bar{\psi}_{ji}$ is specified, thus

$$\bar{\omega}_{ji} = \Delta\xi_k + \Delta\xi_U \tag{28}$$

where Δ is notation that $\Delta = 1$ if the associated variable is ϕ, and $\Delta = i$ if the associated variable is ψ; and k, U are notation for the known and unknown nodal values, respectively. Thus the modelling objective is to reduce $|\Delta\xi_k - \Delta\hat{\xi}_k|$ on Γ.

In the following figures, several potential problems are modelled by the CVBEM. Each problem involves several tries (usually five attempts) to reduce $|\Delta\xi_k - \Delta\hat{\xi}_k|$ on Γ. Because the test problems

have known analytical solutions, the corresponding $|\Delta\xi_U - \Delta\hat{\xi}_U|$ error can be examined also. In general applications, the user does not know this second error distribution and must rely on the boundary condition error exclusively. The test problems do not include sources and sinks as these terms can be approximated exactly by analytical logarithm functions which are simply added to the general approximation solution.

The general procedure for generating the CVBEM solutions is to initially discretize the boundary by nodal points. It can be shown that the density of nodal points is related to the integration accuracy of the approximation. Consequently the user should increase the nodal densities where the trial function assumptions are most inappropriate, such as at boundary angle points and changes in the type of specified boundary condition.

After solving for the approximation function nodal values, the relative error in matching the known boundary conditions is estimated, $\Delta(\hat{\xi}_k - \xi_k)$. At locations of high error, additional nodal points are added on both sides of the maximum error nodal point, and another CVBEM approximation function is generated. In this fashion, nodal points are added on the problem boundary only where needed to reduce the relative error. This type of adaptive integration approach is directly programmed into the software, with a program termination based on the number of attempts (or a relative error tolerance). It should be noted that the $\Delta(\hat{\xi}_k - \xi_k)$ error bound does not apply to the $\Delta(\hat{\xi}_U - \xi_U)$ error variable. However, in order for the total $|\omega(z) - \hat{\omega}(z)|$ error to be reduced, the $\Delta(\hat{\xi}_k - \xi_k)$ must be reduced.

DISCUSSION OF MODELLING RESULTS

Figure 4 shows the modelling results in approximating a complex variable transcendental function. The square domain (Figure 4a) is used with nodal points initially set to be evenly spaced on the problem boundary. After three trials, 12 nodal points were added at locations of large relative error. Figures 4(b) and 4(c) show the corresponding relative error plots for the known relative error values and the associated unknown relative error values. Again, the so-called unknown relative error would actually be unknown for most applications. However, it is seen that working with the available relative error allows the analyst to determine subsequent CVBEM approximation functions which approach the solution to the boundary value problem.

Figures 5, 6 and 7 show the modelling results in approximating various ideal fluid flow situations. Streamlines are superimposed on the problem domains to illustrate the flow patterns. As in Figure 4, the CVBEM is used to develop an approximation function by initially assuming a nodal point distribution of the problem boundary and adding nodes at locations of large known relative error values. From the figures, the known relative error is significantly reduced by using this procedure for adding nodal points. Additionally, the so-called unknown relative error is considerably reduced.

Figures 8 and 9 show other ideal fluid flow patterns which have some modelling difficulties due to singularities. The CVBEM was applied using the nodal placement procedure based on the known relative error. From the figures, the modelling approach can be used to approximate the effects of singularities close to (but exterior of) the problem boundary.

CONCLUSION

The CVBEM provides a means to numerically model two-dimensional potential problems with a high degree of accuracy. Because the CVBEM produces a measure of relative error, the overall modelling error can be directly reduced by using the adaptive integration techniques of selective nodal point addition. Use of the CVBEM to approximate steady-state heat transport problems,

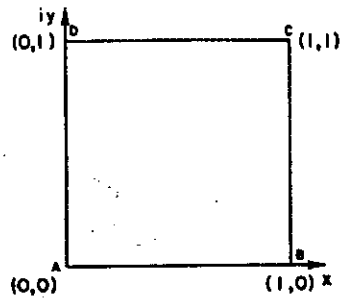

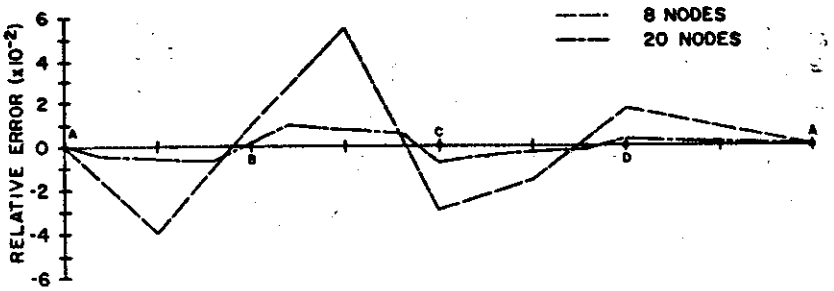

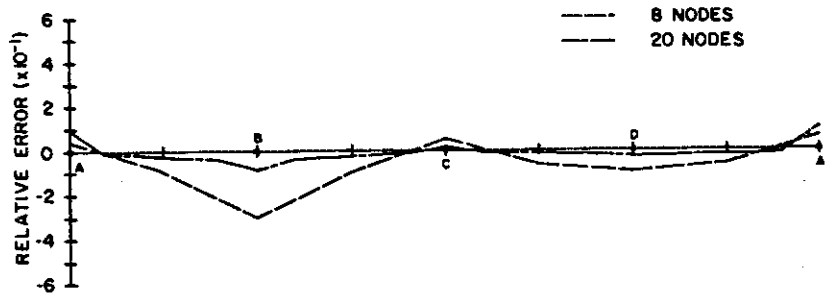

Figure 4. (a) Problem geometry for $W = e^z$; (b) plot of $\Delta(\xi_k - \bar{\xi}_k)$ for $W = e^z$ problem; (c) plot of $\Delta(\xi_u - \bar{\xi}_u)$ for $W = e^z$ problem

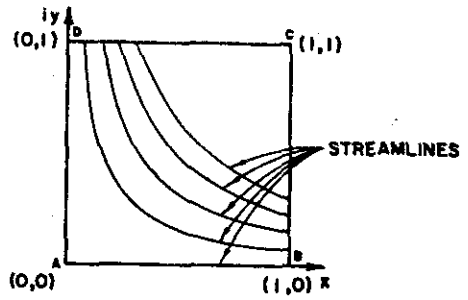

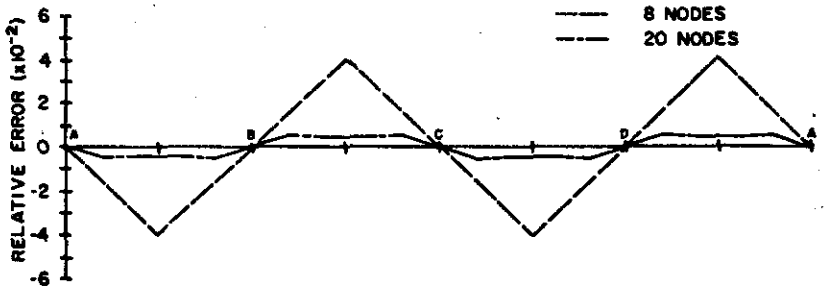

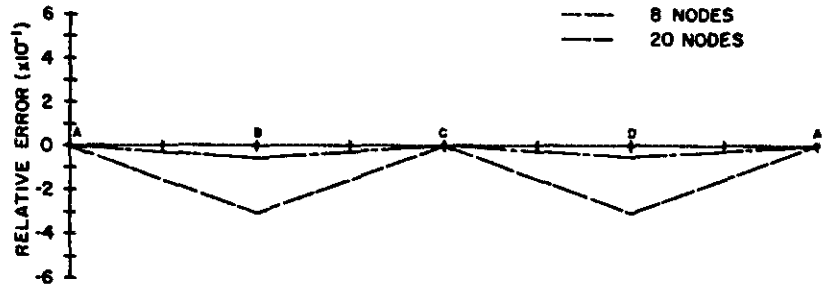

Figure 5. (a) Problem geometry for $W = z^2$ (ideal fluid flow around a corner); (b) plot of $\Delta(\xi_k - \bar{\xi}_k)$ for $W = z^2$ problem; (c) plot of $\Delta(\zeta_k - \bar{\zeta}_k)$ for $W = z^2$ problem

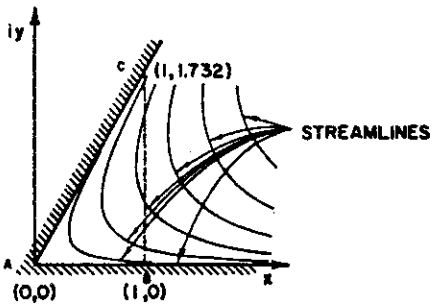

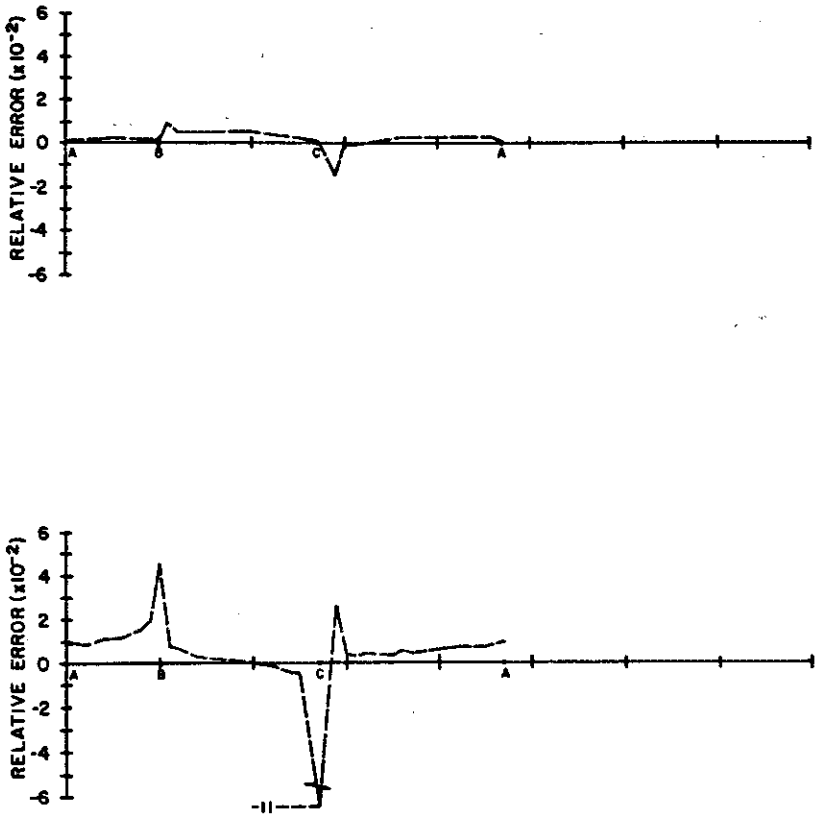

Figure 6. (a)Problem geometry for $W = z^3$ (ideal fluid flow around an angular region); (b) plot of $\Delta(\xi_x - \bar{\xi}_x)$ for $W = z^3$ problem; (c) plot of $\Delta(\xi_y - \bar{\xi}_y)$ for $W = z^3$ problem

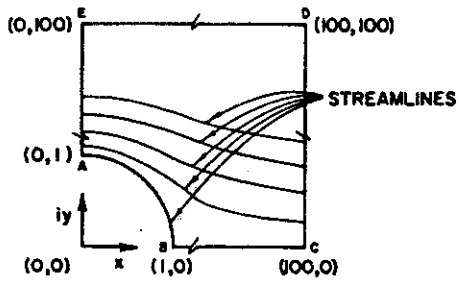

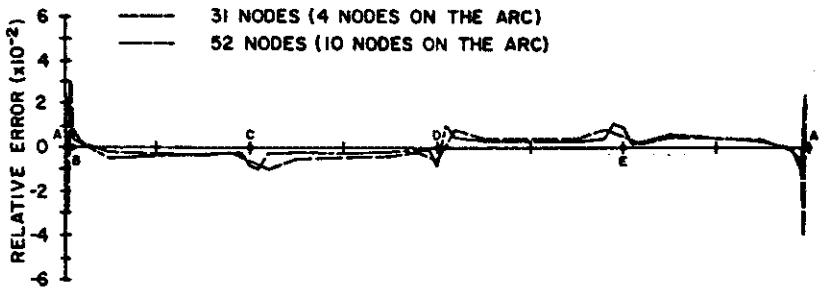

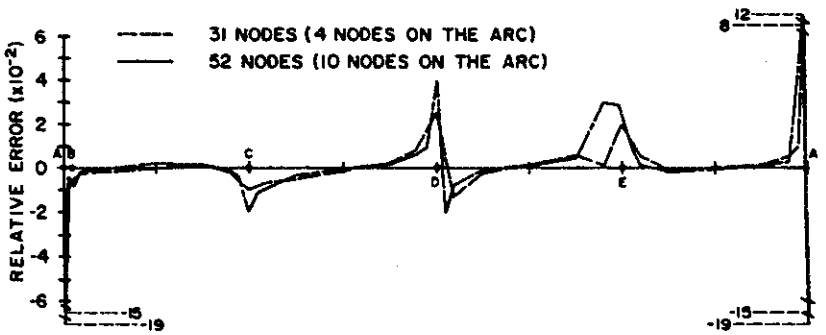

Figure 7. (a) Problem geometry for $W = z + z^{-1}$ (ideal fluid flow over a cylinder); (b) plot of $\Delta(\xi_k - \bar{\xi}_k)$ for $W = z + z^{-1}$ problem; (c) plot of $\Delta(\xi_u - \bar{\xi}_u)$ for $W = z + z^{-1}$ problem

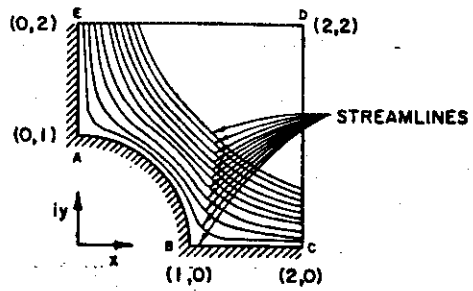

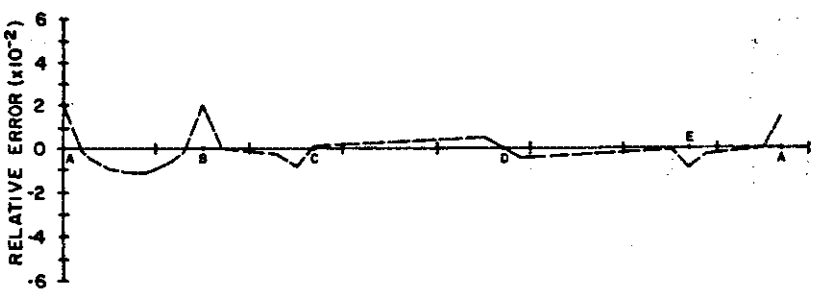

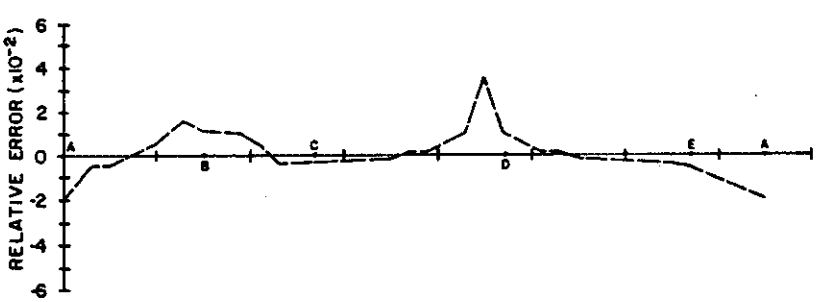

Figure 8. (a) Problem geometry for $W = z^2 + z^{-2}$ (ideal fluid flow around a cylindrical corner); (b) plot of $\Delta(\xi_k - \bar{\xi}_k)$ for $W = z^2 + z^{-2}$ problem; (c) plot $\Delta(\xi_u - \bar{\xi}_u)$ for $W = z^2 + z^{-2}$ problem

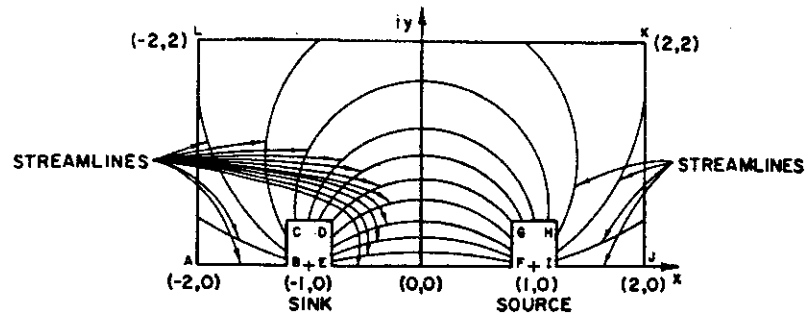

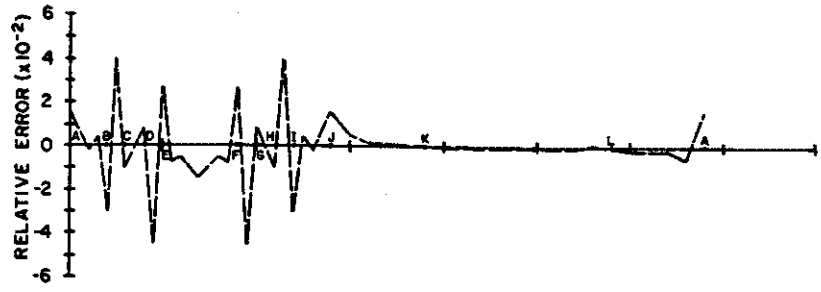

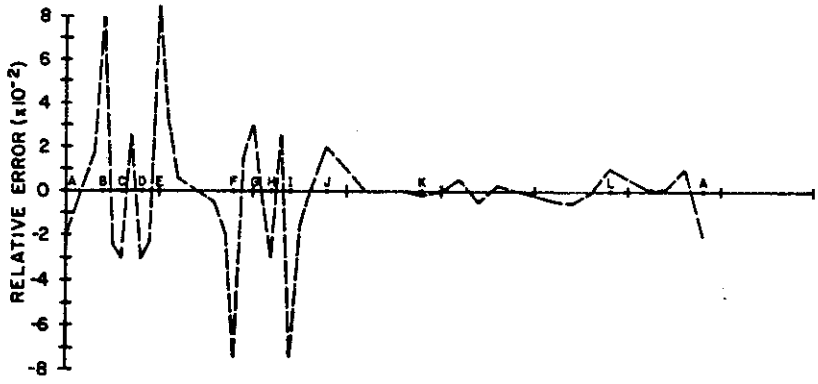

Figure 9. (a) Problem geometry for $W = \log\left(\frac{z-1}{z+1}\right)$ (source and sink of equal strength); (b) plot of $\Delta(\xi_k - \xi_k)$ for $W = \log\left(\frac{z-1}{z+1}\right)$ problem; (c) plot of $\Delta(\xi_u - \xi_u)$ for $W = \log\left(\frac{z-1}{z+1}\right)$ problem

saturated groundwater flow problems, electrostatics and other potential problems is straightforward and requires approximately the same computational effort as other boundary integral approaches.

REFERENCES

1. B. Hunt and L. Isaacs, 'Integral equation formulation for ground-water flow', *A.S.C.E. Hyd. Div.*, **HY10** (1981).
2. T. V. Hromadka II and G. L. Guymon, 'Application of a boundary integral equation to prediction of freezing fronts in soils', *Cold Regions Sci. Technol.*, **6** (1982).
3. T. V. Hromadka II and G. L. Guymon, 'A complex variable boundary element method: development', *Int. numer. methods eng.*, (1984).
4. T. V. Hromadka II, and G. L. Guymon, 'An algorithm to reduce approximation error from the CVBEM', submitted to *Cold Regions Sci. Technol.* (1983).